The Extreme Positive Indian Ocean Dipole of 2019 and Associated Indian Summer Monsoon Rainfall Response

Satyaban B. Ratna[1], Annalisa Cherchi[2,3], Timothy J. Osborn[1], Manoj Joshi[1] and Umakanth Uppara[1]

[1]Climatic Research Unit, School of Environmental Sciences, University of East Anglia, Norwich, NR4 7TJ, United Kingdom

[2]Institute of Atmospheric Sciences and Climate (ISAC-CNR), Bologna, Italy

[3]Istituto Nazionale di Geofisica e Vulcanologia, Bologna, Italy

Corresponding author: Satyaban B. Ratna (S.Bishoyi-Ratna@uea.ac.uk)

Key Points:

- The positive Indian Ocean Dipole event that occurred in 2019 was among the strongest in the modern instrumental record
- The 2019 Indian Summer monsoon exhibited an unusual seasonal evolution with dry conditions in June but resulted in above normal rainfall
- The seasonal evolution of ISM was partly driven by a combination of equatorial Pacific and Indian Ocean sea surface temperature anomalies

Abstract

The positive Indian Ocean Dipole (IOD) event in 2019 was among the strongest on record, while the Indian Summer monsoon (ISM) was anomalously dry in June then very wet by September. We investigated the relationships between the IOD, Pacific sea surface temperature (SST) and ISM rainfall during 2019 with an atmospheric general circulation model forced by observed SST anomalies. The results show that the extremely positive IOD was conducive to a wetter-than-normal ISM, especially late in the season when the IOD strengthened and was associated with anomalous low-level divergence over the eastern equatorial Indian Ocean and convergence over India. However, a warm SST anomaly in the central equatorial Pacific contributed to low level divergence and decreased rainfall over India in June. These results help to better understand the influence of the tropical SST anomalies on the seasonal evolution of ISM rainfall during extreme IOD events.

Plain Language Summary

A prominent pattern of variability in the Indian Ocean is a seesaw in sea surface temperature (SST) between the eastern and western sides of the Ocean basin, called the Indian Ocean Dipole (IOD). Its influence on the regional weather and climate is not yet fully established, but the extremely strong IOD event in 2019 provided us the opportunity to consider its impact on the Indian Summer Monsoon. By simulating the response to the anomalous SST patterns that occurred in 2019, and by observation-based analyses, we find evidence that the IOD did influence the monsoon rainfall in 2019, but that SST anomalies in the Pacific Ocean were also important. Our simulations show that the positive IOD was conducive to wetter-than-normal conditions throughout and especially at the end of the monsoon season, but that anomalous warmth in the central equatorial Pacific may have contributed to reduced rainfall in June over India. The results from this study help to understand the role of SST anomalies within and outside the Indian Ocean in affecting ISM rainfall intensity and seasonal evolution during extreme IOD events.

1 Introduction

The Indian Ocean Dipole (IOD) is one of the dominant modes of variability of the tropical Indian Ocean which was discovered and named at the end of the 1990s (Saji et al 1999; Webster et al 1999). The IOD has been recognized as being forced by ENSO (Allan et al., 2001; Baquero-Bernal et al., 2002; Huang and Kinter, 2002; Dommenget, 2011; Zhao et al., 2019) as well as a self-sustained mode of oscillation (Ashok et al., 2003; Yamagata et al., 2004; Behera et al., 2006), with modelling frameworks supporting both hypotheses (Fischer et al., 2005; Behera et al., 2006; Wang et al., 2019; Cretat et al., 2018). The IOD has also been suggested as a potential trigger for ENSO (Luo et al., 2010; Izumo et al., 2010; Zhou et al., 2015; Jourdain et al., 2016; Wieners et al., 2017; Wang et al., 2019; Cai et al., 2019), with IOD events co-occurring with ENSO that may fasten its phase transition (Kug and Kang, 2006; Kug and Ham, 2012). Past changes in the frequency and in the teleconnections of the IOD have been documented on long time records (e.g. Abram et al., 2020).

The IOD teleconnections span from nearby countries like India (Ashok et al., 2001; Li et al., 2003; Meehl et al., 2003; Wu and Kirtman, 2004; Cherchi et al., 2007; Krishnan et al., 2011; Cherchi and Navarra, 2013; Krishnaswamy et al., 2015; Chowdary et al., 2016; Srivastava et al., 2019, as some examples of the wide published literature available), Indonesia (Pan et al., 2018), Africa (Black et al., 2003; Manatsa and Behera, 2013; Endris et al., 2019) and Australia (i.e., Cai et al., 2009; Ummenhofer et al., 2013; Dey et al., 2019; Hossain et al., 2020), to more remote places, like Brazil (Chan et al., 2008; Taschetto and Ambrizzi, 2012; Bazo et al., 2013).

Here we are particularly interested on the relationship between the IOD and the Indian summer monsoon (ISM). Summer monsoon rainfall over India represents the largest source of annual water for the country (Mall et al., 2006; Archer et al., 2010) and is important for the agrarian economy (Gadgil and Gadgil, 2006; Webster et al, 1998). Despite its annual occurrence, the Indian summer monsoon is highly variable in time and space, with the largest portion of its variability modulated by ENSO, as known since the beginning of the 19th century (Walker, 1924; Sikka, 1980; Rasmusson and Carpenter, 1983; Kirtman and Shukla, 2000; Ratna et al 2011; Sikka and Ratna, 2011, as few examples). Toward the end of the 20th century a weakening of the ISM-ENSO relationship has been identified (Kumar et al., 1999; Kinter et al 2002) with the IOD recognized as a potential trigger of ISM rainfall. Several papers reported the individual and combined influences of ENSO and IOD on ISM rainfall and found that both phenomena, individually and combined, affect ISM rainfall performance

(Ashok et al., 2004; Sikka and Ratna, 2011; Krishnaswamy et al 2015; Li et al., 2017; Hrudya et al 2020).

The active and break spells of monsoons are regulated by the boreal summer intraseasonal oscillation (BSISO), which propagates north from the equator into the Indian monsoon region and substantially affects the monsoon rainfall (Sikka and Gadgil 1980; Sperber et al., 2000). Within the monsoon season, the mean structure of moisture convergence and meridional specific humidity distribution undergoes significant changes in contrasting IOD years, which in turn influences the meridional propagation of BSISO and hence the related precipitation anomalies over India (Ajayamohan et al., 2008; Kikuchi et al., 2012; Singh and Dasgupta, 2017; Konda and Vissa, 2019). At this timescale, the ocean-atmosphere dynamical coupling has been found to be important to the extended Indian summer monsoon break of July 2002 (e.g. Krishnan et al 2006).

Some recent studies have investigated the causes of the strong IOD event in 2019. In particular, it has been found that the occurrence of 2019 extreme pIOD event features the strongest easterly and southerly wind anomalies on record, leading to the strongest wind speed that facilitated the latent cooling to overcome the increased radiative warming over the eastern equatorial Indian Ocean, leading to the unique thermodynamical forcing (Wang et al., 2020). The thermocline warming associated with anomalous ocean downwelling in the southwest tropical Indian Ocean triggered atmospheric convection to induce easterly winds anomaly along the equator and the positive feedbacks led to an IOD event (Du et al., 2020). Also, the record-breaking interhemispheric pressure gradient over the Indo-Pacific region induced northward cross-equatorial flow over the western Maritime Continent, able to trigger strong wind-evaporation-SST and thermocline feedbacks that contributed to the strong IOD (Lu and Ren, 2020). Wang and Cai (2020) described how the consecutive occurrence of positive IDO in 2018 and 2019, along with the evolution of a Central Pacific El Niño, influenced Australian climate. The 2019 IOD event led to unusually warm conditions in many parts of East Asia during 2019–2020 winter (Doi et al 2020), though not necessarily linked with the severe drought that occurred during that fall in East China (Ma et al 2020). In terms of predictability, such an extreme event like the 2019 IOD could be predicted a few seasons in advance (Doi et al., 2020).

In this study we intend to investigate the dynamical aspects of the relationship between IOD and Indian summer monsoon rainfall with a specific focus on 2019. That year was peculiar in terms of the seasonal evolution of precipitation over India with dry conditions at the beginning of the monsoon season and very wet conditions toward the end (Sunitha

Devi et al., 2020). In particular, we designed a set of sensitivity experiments to verify the role of anomalous SST in the Indian Ocean, i.e. the developing IOD that year, and the SST anomalies elsewhere. The work is organized as follows: Section 2 describes the data used for the analysis as well as the model and experiments performed. Section 3 is dedicated to the observed characteristics of IOD and ISM during 2019 with specific attention to the evolution within the summer season. Section 4 shows the results from the sensitivity experiments performed, including a discussion of the main results obtained. Finally, section 5 summarizes the main finding and provide future perspectives from this analysis.

2 Methods

2.1 Observed datasets and indices

The SST anomaly difference between the west (50°E-70°E, 10°S-10°N) and east (90°E-110°E, 10°S-0°) equatorial Indian Ocean, identified as the Dipole Mode Index (DMI; Saji et al., 1999), is used as the metric for the IOD and we computed it using three different datasets: Extended Reconstructed Sea Surface Temperature v5 (ERSST; Huang et al., 2017) available at 2° latitude-longitude degree resolution, National Oceanic and Atmospheric Administration optimum interpolation SST version 2 (NOAA OISSTv2; Reynolds et al., 2002) available at 0.25° resolution, and Hadley Centre Sea Ice and Sea Surface Temperature data set v1.1 (HadISST; Rayner et al., 2003) available at 1° resolution. Other indices used are: Nino3.4 (area averaged SST anomaly over equatorial Pacific, 5°N-5°S 170°W-120°W) from https://psl.noaa.gov/gcos_wgsp/Timeseries/Nino34/ and El Nino-Modoki (Ashok et al., 2007; Weng et al, 2007) from http://www.jamstec.go.jp/virtualearth/general/en/index.html .

For rainfall we used the Global Precipitation Climatology Project (GPCP) data (Adler et al., 2003) available at 2.5° resolution. We also have used the Homogeneous Indian Monthly Rainfall Data Sets (Kothawale and Rajeevan, 2017) from https://tropmet.res.in/static_pages.php?page_id=53. Other atmospheric variables and the global SST field are taken from National Center for Environmental Prediction-Department of Energy (NCEP-DOE) Reanalysis 2 (Kanamitsu et al., 2002) available at 2.5 degree resolution. All anomalies are calculated with respect to the 1981-2010 climatology.

2.2 The IGCM4 model and sensitivity experiments

The Intermediate General Circulation Model version 4 (IGCM4; Joshi et al. 2015) is a global spectral primitive equation atmospheric model with a spectral truncation at T42 (corresponding to 128x64 grid points in the horizontal) and 20 layers in the vertical, with the top at 50 hPa. This configuration, i.e. T42L20, is the standard for studies of the troposphere and climate (Joshi et al. 2015). IGCM4 has been extensively used in climate research, process modelling and atmospheric dynamics (van der Wiel et al., 2016; O' Callaghan et al., 2014; Ratna et al., 2020). The IGCM4 gives a good representation of the mean climate state (Joshi et al, 2015), in particular the simulated climatology and annual cycle over Asia is in reasonable agreement with the reanalysis for temperature and precipitation (Ratna et al., 2020). The physical parameterization schemes used here are the same as in Joshi et al (2015) and Ratna et al (2020).

The set of experiments performed with the IGCM4 consist of a control simulation (CTRL) with prescribed SST obtained from a climatology (1981-2010) of the skin temperature in the NCEP-DOE Reanalysis 2 (Kanamitsu et al, 2002) and two sensitivity experiments where the 2019 SST anomaly is added to the CTRL climatology globally (IODglob) and only over the Indian Ocean (IODreg). All other boundaries conditions are the same as in CTRL. The surface albedo has been adjusted to indicate the presence or absence of sea ice according to whether the new surface temperature was below freezing. We used the greenhouse gas concentration in the model which is close to the 1995 value, the midpoint of the 1981-2010 climatology. For each simulation, the model is integrated for 55 years and the mean of the last 50 years is analysed, excluding the first five years as model spin up. These simulations are long enough to allow a clear separation of the response to the SST anomalies from the internally generated variability, especially for “noisy” variables such as precipitation.

3 2019 Indian Ocean Dipole and Indian Summer Monsoon

The Indian Ocean Dipole (IOD) was unusually strong in 2019 (Fig. 1a). The positive IOD event was the strongest of the last two decades, and possibly the strongest of the last 38 years. The Sep-Nov 2019 DMI was four standard deviations above the 1981-2010 climatology in the ERSST data. This exceeded the previous strong event of 1997 in the ERSST and NOAA-OI-SST datasets, while 1997 remained the strongest in HadISST (Fig. S1). The 2019 positive IOD phase arose from both negative SST anomalies over the eastern equatorial Indian Ocean (EEIO) and warm SST anomalies over the western equatorial Indian Ocean (WEIO) from June to October (Fig 1c-h). However, the evolution of the event was strongly determined by the EEIO, which largely cooled from climatological conditions in

May to almost 1 K cooler than normal by October. On the other hand, the WEIO stayed more constant (i.e. less than 1 K warmer than normal) throughout the period (Fig. 1b).

The total seasonal (June-September) rainfall over India was 110% with respect to its long period average, with the June rainfall quite low (67%) while the September one quite excessive (152%) (Yadav et al., 2020). These conditions have been part of large-scale rainfall anomalies observed in the regions surrounding the Indian Ocean in 2019 (Fig. 2a, d and g). In this study we are interested to understand what anomalous climate conditions within the 2019 summer season contributed to monsoon rainfall variation from a dry June to a wet September over India.

The annual evolution of the IOD index is compared with ENSO associated indices for the year 2019 (Fig 1b). The IOD is strong compared to the rest of indices during 2019 so it is interesting to consider the role of IOD on the seasonal evolution of ISM rainfall. The IOD index intensified from July and reached its peak during October-November (Fig 1b), due to the strengthening of the SST anomaly in the EEIO, as noted above. Nino3.4 SST indicates that ENSO condition was slightly positive in June, before decreasing in strength to reach zero anomaly in September. El Nino Modoki index, which is indicator of a central Pacific SST anomaly, remained slightly above normal throughout the year (Fig. 1c-h).

We have compared (Fig. S2) the seasonal evolution of the IOD, Pacific indices and ISM rainfall (Table S1) with three other strong IOD events (1994, 1997, 2006) to consider if they support our finding that a strengthening positive IOD may be associated with a wetter ISM when not overwhelmed by ENSO influences. In 1994, a positive IOD strengthened further from June to August. Although the central Pacific was warmer than normal, El Nino conditions were not reached, perhaps allowing the IOD to dominate and contribute to above-average ISM rainfall in most months and in the seasonal total (Ashok et al., 2004; Sikka and Ratna, 2011). By contrast, 1997 was dominated by a very strong El Nino, though the expected ENSO-induced anomalous subsidence may have been neutralized/reduced by anomalous IOD-induced convergence over the Bay of Bengal (Behera et al., 1999; Ashok et al, 2001) and contributed to a near-normal ISM season. During 2006, the onset of positive IOD was late compared to the other years considered, perhaps contributing to above normal rainfall in the final months of the ISM (the Modoki index was close to normal and Nino3.4 only warmed to an El Nino state later in the year). Overall, out of these four years, the two with the strongest positive IOD and relatively weak Nino3.4 anomalies (1994 and 2019) had excess ISM rainfall (+15% and +16% with respect to the 1981-2010 climatology, Table S1).

There was a smaller increase in ISM rainfall in 2006 (+9%) when the IOD event developed later, while 1997 had a strong El Nino and a normal ISM season (+2%).

4 Mechanisms contributing to the anomalous 2019 Indian summer monsoon rainfall

To understand the contribution that SST forcing may make to the 2019 rainfall variability over the Indian landmass, we compared the model simulated anomaly (IODglob and IODreg as explained in Section 2) with the observed anomaly. Following the design of the experiments, the comparison is focused in the identification of the rainfall pattern anomalies in the different cases. Of course, we do not expect perfect agreement, even were the model perfect, because of internal atmospheric variability unrelated to the 2019 SST anomalies. Nevertheless, both sensitivity experiments reproduce a dipole precipitation anomaly over the south equatorial Indian Ocean (dry in the east, wet in the west; Fig. 2a-c) during the whole monsoon season (June-September) that closely resembles the observed pattern. Observed Jun-Sep precipitation is above average over the Indian land mass and over the Bay of Bengal, and both experiments simulate a qualitatively similar pattern. Instead, the intensity of the anomaly is larger when the model is forced with only Indian Ocean SST anomalies (IODreg; Fig. 2c) compared to the global SST (IODglob) anomaly (Fig. 2b). This indicates the importance of the 2019 Indian Ocean SST anomaly in contributing to wet conditions over India, though it is modulated by SST anomalies elsewhere.

The comparison of the sensitivity experiments also illuminates on the possible mechanisms behind the two contrasting months of the season (i.e. dry June and wet September). In June, the model response to Indian Ocean SST forcing produces a stronger south-westerly monsoon flow and wet anomalies over western India (IODreg; Fig. 2f), whereas including SST anomalies from other ocean basins (IODglob; Fig. 2e) suppresses the wet anomaly and brings the simulated response closer to the observations (with the exception of the western Indian Ocean). The negative rainfall anomaly over EEIO is also stronger in IODglob compared to IODreg and more similar to the observations. On the other hand, both IODglob and IODreg experiments have a wet anomaly over India in September, as is also seen in the observations (though the observed anomaly is stronger and more extensive). These results indicate that the 2019 Indian Ocean SST anomalies suppress rainfall in the EEIO and favour a wetter than normal Indian monsoon, but that in June the latter is more than offset by a response to the SST anomaly outside the Indian Ocean, resulting in the dry anomaly, as it is observed.

Considering the whole 2019 season, stronger low-level southerly wind anomalies dominated over the Bay of Bengal due to low level divergence over EEIO associated with the very positive IOD (Fig. 2a,b,c). The low-level winds are similar to Behera and Ratnam (2018) where they show low level westerlies and southerlies towards India originated from the EEIO but they do not show any significant cross equatorial flow in their positive IOD events composite. Over the Arabian Sea, the IODreg simulation has stronger south-westerly anomaly compared to IODglob and hence simulates excess rainfall (Fig. 2a, b, c). In June, the dry anomaly observed over India is related to low-level anomalous anticyclonic circulation over central-east India and adjacent Bay of Bengal and to anomalous easterlies prevailing in the peninsular India (Fig 2d). Both circulation features reduced the monsoon flow towards India and hence contributed to the negative rainfall anomaly over India. IODglob realistically simulated both these anomalous circulation features (Fig. 2e), whereas IODreg did not and it shows strong south-westerly flow reaching the Indian landmass (Fig. 2f). In September 2019, observations show that there was a strong anomalous south-westerly flow towards Indian landmass and associated cyclonic circulation over central west India, contributing to the excess rainfall (Fig. 2g). Both sensitivity experiments (Fig. 2h and 2i) simulated anomalously strong south-westerly flow and anomalous cyclonic circulation over India, though they are not as strong as observed.

Consistent with precipitation and low-level wind patterns, there is convergence in the upper troposphere over the Maritime Continent and EEIO in September when the IOD is at its peak (Fig. 3b), but such convergence does not appear in June (Fig. 3a) when the IOD is developing and there are still warm SST anomalies over the equatorial Pacific (Fig. 1). In the IODglob experiment (Fig. 3c) we see that the model responds strongly to these equatorial Pacific SST anomalies in June, causing strong upper level divergence over east equatorial Pacific and convergence over the Maritime Continent. The opposite circulation is seen at lower levels (see Fig. S2 for the 850 hPa velocity potential and divergent winds) which causes low level divergence extending from the Maritime Continent to the Bay of Bengal and Indian landmass, contributing to negative rainfall anomaly in June. In IODreg, where the model is forced with the 2019 SST anomaly only over the Indian Ocean, the model responds with upper level (lower level) divergence (convergence) over the Indian Ocean and over India (extending from Australia via WEIO to India; Fig. 3e and S2), which would have contributed to a positive rainfall anomaly in June. The model simulated velocity potential anomaly explains the model simulated rainfall and its link with Indian Ocean and Pacific Ocean SST anomaly, and indicates that the response is more closely linked with the equatorial Pacific SST rather with the SST anomalies in the extratropical North Pacific which were also large in 2019. Both sensitivity experiments simulate upper level divergence over

EEIO region in September, although in IODglob it is stronger than in IODreg, and this explains the link between the Indian Ocean SST anomaly and the circulation and rainfall anomalies.

5 Conclusions

One of the strongest positive IOD events in the historical period occurred in 2019. The evolution of the 2019 IOD was characterized by a cold anomaly over the EEIO which started strengthening from June and reached its peak in October, remaining strong until November. In the same year, the Indian summer monsoon season experienced peculiar behaviour with weak rainfall during June (despite the IOD index being already in its positive phase). Then the monsoon gained its strength from July, ending with an anomalous wet September and contributing to above-normal seasonal rainfall.

With a suite of atmospheric GCM experiments we have been able to evidence the role of the IOD and of the SST anomalies elsewhere in the seasonal evolution of rainfall and circulation anomalies during the 2019 summer monsoon. The anomalous SST gradient between the west and east equatorial Indian Ocean drives a dipole in equatorial precipitation anomalies and anomalous low-level circulation that would, in isolation, lead to a wetter than normal Indian summer monsoon across the monsoon season including June and September. However, when forcing the IGCM4 model with the global pattern of SST anomalies observed in 2019, the response changes, particularly in June. Although not considered to be an El Nino, the first half of 2019 did exhibit anomalously warm conditions in the central Pacific (visible in the Nino3.4 index) that dissipated by September. The model responds to this equatorial Pacific warmth with upper-level divergence over the equatorial Pacific and convergence over the Maritime Continent. This causes low-level divergence extending from the Maritime Continent to the Bay of Bengal and the Indian landmass, contributing to a negative rainfall anomaly there in June. By September, this response to remote forcing from the Pacific weakens (likely linked in part to the weakening of the Nino3.4 SST anomaly there), leaving the response to the Indian Ocean SST anomalies (linked to the very strong IOD) to dominate. This response arises from strong IOD-related low-level divergence over EEIO and convergence over the Indian landmass, contributing to excessive rainfall.

The similarity between the model simulations and observed/reanalysis data provides evidence that these mechanisms occurred in the real world in 2019, i.e. that there was a contrasting contribution from the Pacific and Indian Ocean SST anomalies to ISM rainfall. The tropical Pacific SST contributed to a drying tendency over India while the IOD contributed to anomalous wet conditions over India. The Pacific effect dominated in June, contributing to the dry anomalies observed, but the weakening Pacific SST anomalies and especially the dramatic strengthening of the IOD led to the latter dominating by September and having a significant contribution to the very wet September observed.

The observed June and September rainfall anomalies were more extreme than those simulated in these SST-forced experiments, reinforcing the role that internal atmospheric variability plays in any particular month or season. Nevertheless, the results from this study help to understand the role of SST anomalies within and outside the Indian Ocean in affecting ISM rainfall intensity and seasonal evolution during extreme IOD events. This is important for improving seasonal predictions of Indian summer monsoon, and our results also highlight that, to predict the seasonal evolution of ISM rainfall, Pacific SST anomalies must be considered even when there is an extremely strong IOD. For example, Li et al (2017) show that the majority of CMIP5 models simulate an unrealistic present-day IOD-ISMR correlation due to an overly strong control by ENSO and hence a positive IOD is associated with a reduction of ISM rainfall in the simulated present-day climate. Hence, coupled climate models need to improve their simulation of these type of linkages.

Acknowledgements

This study is supported by the Belmont Forum and JPI-Climate project INTEGRATE (An Integrated data-model study of interactions between tropical monsoons and extratropical climate variability and extremes) with funding by UK NERC grant NE/P006809/1. The model experiments were conducted on the High Performance Compute Cluster at the University of East Anglia. We thank the two anonymous reviewers for their constructive comments.

Data Availability Statement

The data used in this study can be downloaded from the following websites:

ERSST (https://psl.noaa.gov/data/gridded/data.noaa.ersst.v5.html);
OISST (https://psl.noaa.gov/data/gridded/data.noaa.oisst.v2.html);
HadISST (https://www.metoffice.gov.uk/hadobs/hadisst/);
GPCP (https://psl.noaa.gov/data/gridded/data.gpcp.html);
NCEP-DOE Reanalysis 2 (https://psl.noaa.gov/data/gridded/data.ncep.reanalysis2.html)
Nino3.4 (https://psl.noaa.gov/gcos_wgsp/Timeseries/Nino34/);
El Niño Modoki (http://www.jamstec.go.jp/virtualearth/general/en/index.html);

Indian Monthly Rainfall Data (https://tropmet.res.in/static_pages.php?page_id=53);
The model used in this study is described in (Joshi et al. 2015; https://gmd.copernicus.org/articles/8/1157/2015/)

References

Abram, N. J., Wright, N. M., Ellis, B., Dixon, B. C., Wurtzel, J. B., England, M. H., et al. (2020). Coupling of Indo-Pacific climate variability over the last millennium. Nature, 579, 385-392. https://doi.org/10.1038/s41586-020-2084-4

Adler, R. F., Huffman, G. J., Chang, A., Ferraro, R., Xie, P. P., Janowiak, J., et al. (2003). The version-2 global precipitation climatology project (GPCP) monthly precipitation analysis (1979-present). Journal of Hydrometeorology. https://doi.org/10.1175/1525-7541(2003)004<1147:TVGPCP>2.0.CO;2

Ajayamohan, R. S., Rao, S. A. & Yamagata, T. (2008). Influence of Indian Ocean Dipole on Poleward Propagation of Boreal Summer Intraseasonal Oscillations. J. Climate, 21, 5437–5454, https://doi.org/10.1175/2008JCLI1758.1.

Allan, R. J., Chambers, D., Drosdowsky, W., Hendon, H., Latif, M., Nicholls, N., et al. (2001). Is there an Indian Ocean dipole and is it independent of the El Niño-Southern Oscillation? CLIVAR Exchanges, 6, 18–22.

Archer, D. R., Forsythe, N., Fowler, H. J., & Shah, S. M. (2010). Sustainability of water resources management in the Indus Basin under changing climatic and socio economic conditions. Hydrology and Earth System Sciences, 14(8):1669–80. https://doi.org/10.5194/hess-14-1669-2010

Ashok, K., Behera, S. K., Rao, S. A., Weng, H., & Yamagata, T. (2007). El Niño Modoki and its possible teleconnection. Journal of Geophysical Research: Oceans, 112, C11007. https://doi.org/10.1029/2006JC003798

Ashok, K., Guan, Z., & Yamagata, T. (2001). Impact of the Indian Ocean dipole on the relationship between the Indian monsoon rainfall and ENSO. Geophysical Research Letters, 28, 4499-4502. https://doi.org/10.1029/2001GL013294

Ashok, K., Guan, Z., & Yamagata, T. (2003). A look at the relationship between the ENSO and the Indian Ocean Dipole. Journal of the Meteorological Society of Japan, 81, 41-56. https://doi.org/10.2151/jmsj.81.41

Ashok, K., Guan, Z., Saji, N. H., & Yamagata, T. (2004). Individual and combined influences of ENSO and the Indian Ocean Dipole on the Indian summer monsoon. Journal of Climate. https://doi.org/10.1175/1520-0442(2004)017<3141:IACIOE>2.0.CO;2

Baquero-Bernal, A., Latif, M., & Legutke, S. (2002). On dipolelike variability of sea surface temperature in the tropical Indian Ocean. Journal of Climate, 15, 1358-1368. https://doi.org/10.1175/1520-0442(2002)015<1358:ODVOSS>2.0.CO;2

Bazo, J., Lorenzo, M. D. L. N., & Porfirio Da Rocha, R. (2013). Relationship between monthly rainfall in NW peru and tropical sea surface temperature. Advances in Meteorology. https://doi.org/10.1155/2013/152875

Behera, S. K., & Ratnam, J. V. (2018). Quasi-asymmetric response of the Indian summer monsoon rainfall to opposite phases of the IOD. Scientific Reports. https://doi.org/10.1038/s41598-017-18396-6

Behera, S. K., Luo, J. J., Masson, S., Rao, S. A., Sakuma, H., & Yamagata, T. (2006). A CGCM study on the interaction between IOD and ENSO. Journal of Climate, 19, 1608-1705. https://doi.org/10.1175/JCLI3797.1

Black, E., Slingo, J., & Sperber, K. R. (2003). An observational study of the relationship between excessively strong short rains in coastal East Africa and Indian ocean SST. Monthly Weather Review, 31, 74-94. https://doi.org/10.1175/1520-0493(2003)131<0074:AOSOTR>2.0.CO;2

Cai, W., Cowan, T., & Raupach, M. (2009). Positive Indian Ocean Dipole events precondition southeast Australia bushfires, *Geophys. Res. Lett.*, **36**, L19710, doi: 10.1029/2009GL039902Cai, W., Wu, L., Lengaigne, M., Li, T., McGregor, S., Kug, J. S., et al. (2019). Pantropical climate interactions. Science, 363, 6430. https://doi.org/10.1126/science.aav4236

Chan, S. C., Behera, S. K., & Yamagata, T. (2008). Indian Ocean Dipole influence on South American rainfall. Geophysical Research Letters, 35, L14S12. https://doi.org/10.1029/2008GL034204

Cherchi, A., & Navarra, A. (2013). Influence of ENSO and of the Indian Ocean Dipole on the Indian summer monsoon variability. Climate Dynamics, 41, 81-103. https://doi.org/10.1007/s00382-012-1602-y

Cherchi, A., Gualdi, S., Behera, S., Luo, J. J., Masson, S., Yamagata, T., & Navarra, A. (2007). The influence of tropical Indian Ocean SST on the Indian summer monsoon. In Journal of Climate, 20, 3083-3105. https://doi.org/10.1175/JCLI4161.1

Chowdary, J. S., Parekh, A., Kakatkar, R., Gnanaseelan, C., Srinivas, G., Singh, P., & Roxy, M. K. (2016). Tropical Indian Ocean response to the decay phase of El Niño in a coupled model and associated changes in south and east-Asian summer monsoon circulation and rainfall. Climate Dynamics, 47, 831-844. https://doi.org/10.1007/s00382-015-2874-9

Crétat, J., Terray, P., Masson, S., & Sooraj, K. P. (2018). Intrinsic precursors and timescale of the tropical Indian Ocean Dipole: insights from partially decoupled numerical experiment. Climate Dynamics, 51, 1311-1352. https://doi.org/10.1007/s00382-017-3956-7

Dey, R., Lewis, S. C., & Abram, N. J. (2019). Investigating observed northwest Australian rainfall trends in Coupled Model Intercomparison Project phase 5 detection and attribution experiments. International Journal of Climatology, 39, 112-127. https://doi.org/10.1002/joc.5788

Doi, T., Behera, S. K., & Yamagata, T. (2020). Predictability of the Super IOD Event in 2019 and Its Link With El Niño Modoki. Geophysical Research Letters, 47. https://doi.org/10.1029/2019GL086713

Doi, T., Behera, S. K., & Yamagata, T. (2020). Wintertime impacts of the 2019 super IOD on East Asia. Geophysical Research Letters, 47, e2020GL089456. https://doi.org/10.1029/2020GL089456

Dommenget, D. (2011). An objective analysis of the observed spatial structure of the tropical Indian Ocean SST variability. Climate Dynamics, 36, 2129-2145. https://doi.org/10.1007/s00382-010-0787-1

Du, Y., Zhang, Y., Zhang, L.-Y., Tozuka, T., Ng, B., & Cai, W. (2020). Thermocline warming induced extreme Indian Ocean dipole in 2019. Geophysical Research Letters, 47, e2020GL090079, https://doi.org/10.1029/2020GL090079

Endris, H. S., Lennard, C., Hewitson, B., Dosio, A., Nikulin, G., & Artan, G. A. (2019). Future changes in rainfall associated with ENSO, IOD and changes in the mean state over Eastern Africa. Climate Dynamics, 52, 2029-2053. https://doi.org/10.1007/s00382-018-4239-7

Fischer, A. S., Terray, P., Guilyardi, E., Gualdi, S., & Delecluse, P. (2005). Two independent triggers for the Indian Ocean dipole/zonal mode in a coupled GCM. Journal of Climate, 18(17), 3428–3449. https://doi.org/10.1175/JCLI3478.1

Gadgil, S., & Gadgil, S. (2006). The Indian monsoon, GDP and agriculture. Economic & Political Weekly, 41(47): 4887–4895.

Hossain, I., Rasel, H. M., Imteaz, M. A., & Mekanik, F. (2020). Long-term seasonal rainfall forecasting using linear and non-linear modelling approaches: a case study for Western Australia. Meteorology and Atmospheric Physics, 132, 131-141. https://doi.org/10.1007/s00703-019-00679-4

Hrudya, P. H., Varikoden, H., & Vishnu, R. (2020). A review on the Indian summer monsoon rainfall, variability and its association with ENSO and IOD. Meteorology and Atmospheric Physics. https://doi.org/10.1007/s00703-020-00734-5

http://imdpune.gov.in/Clim_Pred_LRF_New/Reports/Monsoon_Report_2019/Chapter_9.pdf

Huang, Bohua. (2002). Interannual variability in the tropical Indian Ocean. Journal of Geophysical Research, 107 (C11). https://doi.org/10.1029/2001jc001278

Huang, Boyin, Thorne, P. W., Banzon, V. F., Boyer, T., Chepurin, G., Lawrimore, J. H., et al. (2017). Extended reconstructed Sea surface temperature, Version 5 (ERSSTv5): Upgrades, validations, and intercomparisons. Journal of Climate. https://doi.org/10.1175/JCLI-D-16-0836.1

Izumo, T., Vialard, J., Lengaigne, M., De Boyer Montegut, C., Behera, S. K., Luo, J. J., et al. (2010). Influence of the state of the Indian Ocean Dipole on the following years El Nĩo. Nature Geoscience, 3, 168-172. https://doi.org/10.1038/ngeo760

Joshi, M., Stringer, M., Van Der Wiel, K., O'Callaghan, A., & Fueglistaler, S. (2015). IGCM4: A fast, parallel and flexible intermediate climate model. Geoscientific Model Development. https://doi.org/10.5194/gmd-8-1157-2015

Jourdain, N. C., Lengaigne, M., Vialard, J., Izumo, T., & Gupta, A. Sen. (2016). Further insights on the influence of the Indian Ocean dipole on the following year's ENSO from observations and CMIP5 models. Journal of Climate, 29, 637-658. https://doi.org/10.1175/JCLI-D-15-0481.1

Kanamitsu, M., Ebisuzaki, W., Woollen, J., Yang, S. K., Hnilo, J. J., Fiorino, M., & Potter, G. L. (2002). NCEP-DOE AMIP-II reanalysis (R-2). Bulletin of the American Meteorological Society, 83, 1631–1643. https://doi.org/10.1175/bams-83-11-1631

Kikuchi, K., Wang, B. & Kajikawa, Y. (2012). Bimodal representation of the tropical intraseasonal oscillation. *Clim Dyn* **38,** 1989–2000. https://doi.org/10.1007/s00382-011-1159-1

Kinter, I. L., Miyakoda, K., & Yang, S. (2002). Recent change in the connection from the Asian monsoon to ENSO. Journal of Climate, 15, 1203-1215. https://doi.org/10.1175/1520-0442(2002)015<1203:RCITCF>2.0.CO;2

Kirtman, B. P., & Shukla, J. (2000). Influence of the Indian summer monsoon on ENSO. Quarterly Journal of the Royal Meteorological Society, 126, 213-239. https://doi.org/10.1002/qj.49712656211

Konda, G. &Vissa, N.K. (2019). Intraseasonal Convection and Air–Sea Fluxes Over the Indian Monsoon Region Revealed from the Bimodal ISO Index. *Pure Appl. Geophys*. **176,** 3665–3680. https://doi.org/10.1007/s00024-019-02119-1

Kothawale D.R. & Rajeevan M., (2017) Monthly, Seasonal and Annual Rainfall Time Series for All India, Homogeneous Regions and Meteorological Subdivisions: 1871-2016, IITM Research Report No. RR-138.Krishnan, R., Ayantika, D. C., Kumar, V., & Pokhrel, S. (2011). The long-lived monsoon depressions of 2006 and their linkage with the Indian Ocean Dipole. International Journal of Climatology, 31, 1334-1352. https://doi.org/10.1002/joc.2156

Krishnan, R., K. Ramesh, V., Samala, B. K., Meyers, G., Slingo, J. M. & Fennessy, M. J. (2006). Indian Ocean-monsoon coupled interactions and impending monsoon droughts, Geophys. Res. Lett., 33, L08711, doi:10.1029/2006GL025811.

Krishnaswamy, J., Vaidyanathan, S., Rajagopalan, B., Bonell, M., Sankaran, M., Bhalla, R. S., & Badiger, S. (2015). Non-stationary and non-linear influence of ENSO and Indian Ocean Dipole on the variability of Indian monsoon rainfall and extreme rain events. Climate Dynamics, 45, 175-184. https://doi.org/10.1007/s00382-014-2288-0

Kug, J. S., & Ham, Y. G. (2012). Indian ocean feedback to the ENSO transition in a multimodel ensemble. Journal of Climate, 25, 6942-6957. https://doi.org/10.1175/JCLI-D-12-00078.1

Kug, J. S., Kirtman, B. P., & Kang, I. S. (2006). Interactive feedback between ENSO and the Indian Ocean in an interactive ensemble coupled model. Journal of Climate, 19, 1784-1801. https://doi.org/10.1175/JCLI3980.1

Kumar, K. K., Rajagopalan, B., & Cane, M. A. (1999). On the weakening relationship between the indian monsoon and ENSO. Science, 284, 2156-2159. https://doi.org/10.1126/science.284.5423.2156

Li, T., Wang, B., Chang, C. P., & Zhang, Y. (2003). A theory for the Indian Ocean dipole-zonal mode. Journal of the Atmospheric Sciences, 60, 2119-2135. https://doi.org/10.1175/1520-0469(2003)060<2119:ATFTIO>2.0.CO;2

Li, Z., Lin, X. & Cai, W. (2017). Realism of modelled Indian summer monsoon correlation with the tropical Indo-Pacific affects projected monsoon changes. Scientific Reports, 7, 4929. https://doi.org/10.1038/s41598-017-05225-z

Lu, B., & Ren, H. L. (2020). What Caused the Extreme Indian Ocean Dipole Event in 2019? Geophysical Research Letters, 47, e2020GL087768. https://doi.org/10.1029/2020GL087768

Luo, J. J., Zhang, R., Behera, S. K., Masumoto, Y., Jin, F. F., Lukas, R., & Yamagata, T. (2010). Interaction between El Niño and extreme Indian Ocean dipole. Journal of Climate, 23, 726-742. https://doi.org/10.1175/2009JCLI3104.1

Ma, S. M., C. W. Zhu, & J. Liu. (2020). Combined impacts of warm central equatorial Pacific sea surface temperatures and anthropogenic warming on the 2019 severe drought in East China. Adv. Atmos. Sci., 37(11), 1149−1163, https://doi.org/10.1007/s00376-020-0077-8.

Mall, R. K., Gupta, A., Singh, R., Singh, R. S., & Rathore, L. S. (2006). Water resources and climate change: An Indian perspective. Current Science, 90(12):1610–26.

Manatsa, D., & Behera, S. K. (2013). On the epochal strengthening in the relationship between rainfall of East Africa and IOD. Journal of Climate, 26, 5655-5673. https://doi.org/10.1175/JCLI-D-12-00568.1

Meehl, G. A., Arblaster, J. M., & Loschnigg, J. (2003). Coupled ocean-atmosphere dynamical processes in the tropical Indian and Pacific Oceans and the TBO. Journal of Climate, 16, 2138-2158. https://doi.org/10.1175/2767.1

O'Callaghan, A., Joshi, M., Stevens, D., & Mitchell, D. (2014). The effects of different sudden stratospheric warming types on the ocean. Geophysical Research Letters. https://doi.org/10.1002/2014GL062179

Pan, X., Chin, M., Ichoku, C. M., & Field, R. D. (2018). Connecting Indonesian Fires and Drought With the Type of El Niño and Phase of the Indian Ocean Dipole During 1979–2016. Journal of Geophysical Research: Atmospheres, 123, 7974–7988. https://doi.org/10.1029/2018JD028402

Rasmusson, E. M., & Carpenter, T. H. (1983). The relationship between eastern equatorial Pacific sea surface temperatures and rainfall over India and Sri Lanka. Monthly Weather Review, 111, 517-528. https://doi.org/10.1175/1520-0493(1983)111<0517:TRBEEP>2.0.CO;2

Ratna, Satyaban B., Osborn, T. J., Joshi, M., & Luterbacher, J. (2020). The influence of atlantic variability on asian summer climate is sensitive to the pattern of the sea surface temperature anomaly. Journal of Climate, 33, 7567–7590. https://doi.org/10.1175/JCLI-D-20-0039.1

Ratna, Satyaban Bishoyi, Sikka, D. R., Dalvi, M., & Venkata Ratnam, J. (2011). Dynamical simulation of Indian summer monsoon circulation, rainfall and its interannual variability using a high resolution atmospheric general circulation model. International Journal of Climatology, 31, 1927-1942. https://doi.org/10.1002/joc.2202

Rayner, N. A., Parker, D. E., Horton, E. B., Folland, C. K., Alexander, L. V., Rowell, D. P., et al. (2003). Global analyses of sea surface temperature, sea ice, and night marine air temperature since the late nineteenth century. Journal of Geophysical Research: Atmospheres. https://doi.org/10.1029/2002jd002670

Reynolds, R. W., Smith, T. M., Liu, C., Chelton, D. B., Casey, K. S., & Schlax, M. G. (2007). Daily high-resolution-blended analyses for sea surface temperature. Journal of Climate. https://doi.org/10.1175/2007JCLI1824.1

Saji, N. H., Goswami, B. N., Vinayachandran, P. N., & Yamagata, T. (1999). A dipole mode in the tropical Indian ocean. Nature, 401, 360-363. https://doi.org/10.1038/43854

Sikka, D. R. (1980). Some aspects of the large scale fluctuations of summer monsoon rainfall over India in relation to fluctuations in the planetary and regional scale circulation parameters. Proceedings of the Indian Academy of Sciences - Earth and Planetary Sciences, 89, 179-195. https://doi.org/10.1007/BF02913749

Sikka, D. R., & Gadgil, S (1980), On the maximum cloud zone and the ITCZ over Indian longitudes during the southwest monsoon, Mon. Weather Rev., 108, 1840– 1853.

Sikka, D. R., & Ratna, S. B. (2011). On improving the ability of a high-resolution atmospheric general circulation model for dynamical seasonal prediction of the extreme seasons of the Indian summer monsoon. Mausam, 62 (3), 339-360.

Singh C & Dasgupta P (2017). Unraveling the spatio-temporal structure of the atmospheric and oceanic intra-seasonal oscillations during the contrasting monsoon seasons. Atm Res 192 48-57 https://doi.org/10.1016/j.atmosres.2017.03.020

Sperber, K. R., Slingo, J. M., & Annamalai, H. (2000)., Predictability and relationship between subseasonal and interannual variability during the Asian summer monsoon, Q. J. R. Meteorol. Soc., 126, 2545– 2574.

Srivastava, A., Pradhan, M., Goswami, B. N., & Rao, S. A. (2019). Regime shift of Indian summer monsoon rainfall to a persistent arid state: external forcing versus internal variability. Meteorology and Atmospheric Physics, 131, 211-224. https://doi.org/10.1007/s00703-017-0565-2

Taschetto, A. S., & Ambrizzi, T. (2012). Can Indian Ocean SST anomalies influence South American rainfall? Climate Dynamics, 38, 1615-1628. https://doi.org/10.1007/s00382-011-1165-3

Ummenhofer, C. C., Schwarzkopf, F. U., Meyers, G., Behrens, E., Biastoch, A., & Böning, C. W. (2013). Pacific ocean contribution to the asymmetry in eastern indian ocean variability. Journal of Climate, 26, 1152-1171. https://doi.org/10.1175/JCLI-D-11-00673.1

van der Wiel, K., Matthews, A. J., Joshi, M. M., & Stevens, D. P. (2016). The influence of diabatic heating in the South Pacific Convergence Zone on Rossby wave propagation and the mean flow. Quarterly Journal of the Royal Meteorological Society. https://doi.org/10.1002/qj.2692

Walker, G. T. (1924). Correlation in seasonal variations of weather - A further study of world weather. Mon. Wea. Rev., 53, 252–254, https://doi.org/10.1175/1520-0493(1925)53<252:CISVOW>2.0.CO;2.

Wang, G., Cai, W. (2020) Two-year consecutive concurrences of positive Indian Ocean Dipole and Central Pacific El Nino preconditioned the 2019/2020 Australian "black summer" bushfires. Geosci. Lett. 7, 19. https://doi.org/10.1186/s40562-020-00168-2

Wang, G., Cai, W., Yang, K., Santoso, A., & Yamagata, T. (2020). A Unique Feature of the 2019 Extreme Positive Indian Ocean Dipole Event. Geophysical Research Letters, 47, e2020GL088615. https://doi.org/10.1029/2020GL088615

Wang, H., Kumar, A., Murtugudde, R., Narapusetty, B., & Seip, K. L. (2019). Covariations between the Indian Ocean dipole and ENSO: a modeling study. Climate Dynamics, 53, 5743-5761. https://doi.org/10.1007/s00382-019-04895-x

Webster, P. J., Magaña, V. O., Palmer, T. N., Shukla, J., Tomas, R. A., Yanai, M., & Yasunari, T. (1998). Monsoons: processes, predictability, and the prospects for prediction. Journal of Geophysical Research: Oceans, 103(C7):. https://doi.org/10.1029/97jc02719

Webster, Peter J., Moore, A. M., Loschnigg, J. P., & Leben, R. R. (1999). Coupled ocean-atmosphere dynamics in the Indian Ocean during 1997-98. Nature, 401, 356-360. https://doi.org/10.1038/43848

Weng, H., Ashok, K., Behera, S. K., Rao, S. A., & Yamagata, T. (2007). Impacts of recent El Niño Modoki on dry/wet conditions in the Pacific rim during boreal summer. Climate Dynamics, 29(2–3), 113–129. https://doi.org/10.1007/s00382-007-0234-0

Wieners, C. E., Dijkstra, H. A., & de Ruijter, W. P. M. (2017). The influence of the Indian Ocean on ENSO stability and flavor. Journal of Climate, 30, 2601-2620. https://doi.org/10.1175/JCLI-D-16-0516.1

Wu, R., & Kirtman, B. P. (2004). Impacts of the Indian Ocean on the Indian Summer Monsoon-ENSO relationship. Journal of Climate, 17, 3037-3054. https://doi.org/10.1175/1520-0442(2004)017<3037:IOTIOO>2.0.CO;2

Yadav, B.P., Srivastava, A. K., Guhathakurtha, P., Das, A. K., & Manik, S.K. (2020). Regional characteristics of the 2019 southwest monsoon, Monsoon 2019 – A Report. IMD Met Monograph: ESSO/IMD/Synoptic Met/02(2019)/24.

Yamagata, T., Behera, S. K., Luo, J. J., Masson, S., Jury, M. R., & Rao, S. A. (2004). Coupled ocean-atmosphere variability in the tropical Indian ocean. Geophysical Monograph Series, 147, 189–211. https://doi.org/10.1029/147GM12

Zhao, S., Jin, F. F., & Stuecker, M. F. (2019). Improved Predictability of the Indian Ocean Dipole Using Seasonally Modulated ENSO Forcing Forecasts. Geophysical Research Letters, 46, 9980-9990. https://doi.org/10.1029/2019GL084196

Zhou, Q., Duan, W., Mu, M., & Feng, R. (2015). Influence of positive and negative Indian Ocean Dipoles on ENSO via the Indonesian Throughflow: Results from sensitivity experiments. Advances in Atmospheric Sciences, 32, 783-793. https://doi.org/10.1007/s00376-014-4141-0

Figures:

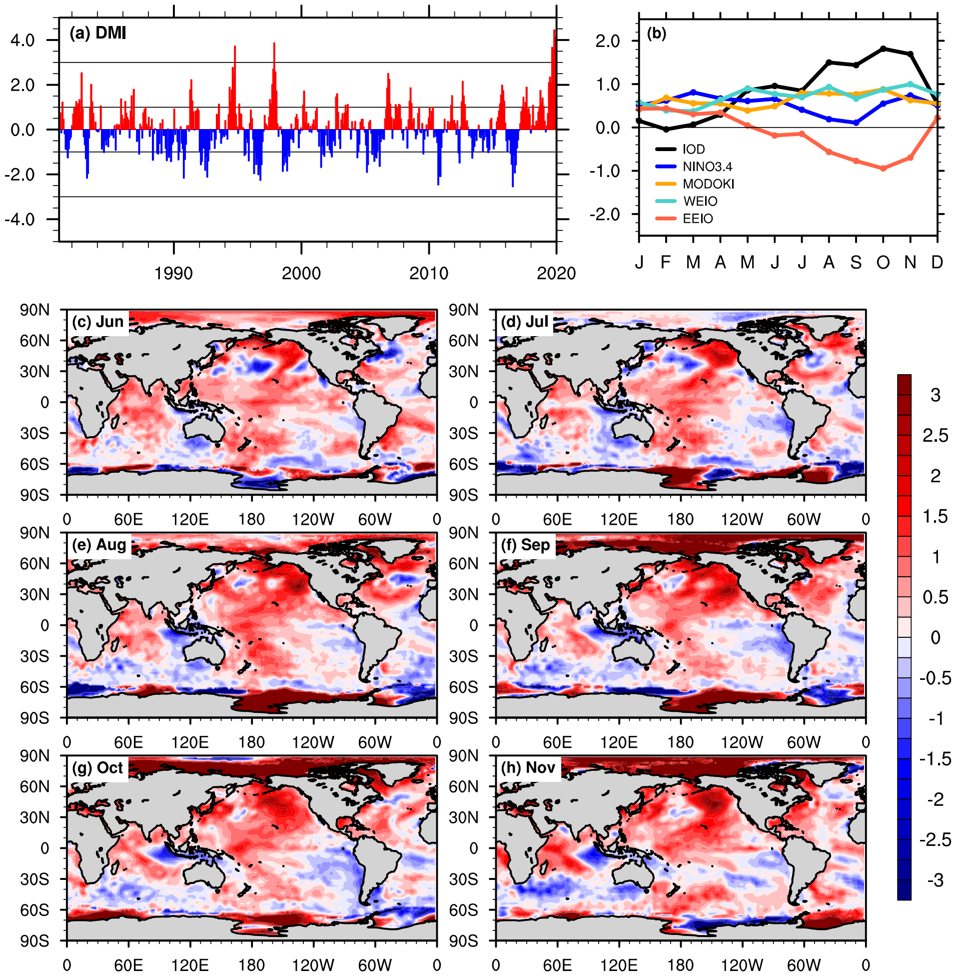

Fig. 1: (a) Standardized monthly Dipole Mode Index (DMI) from 1980 to 2019 calculated using ERSST data. (b) Annual cycle of Indian and Pacific Oceans climate indices (K) for 2019 (as discussed in Section 2). (c-h) Observed 2019 SST anomalies from June to November using NCEP2 data.

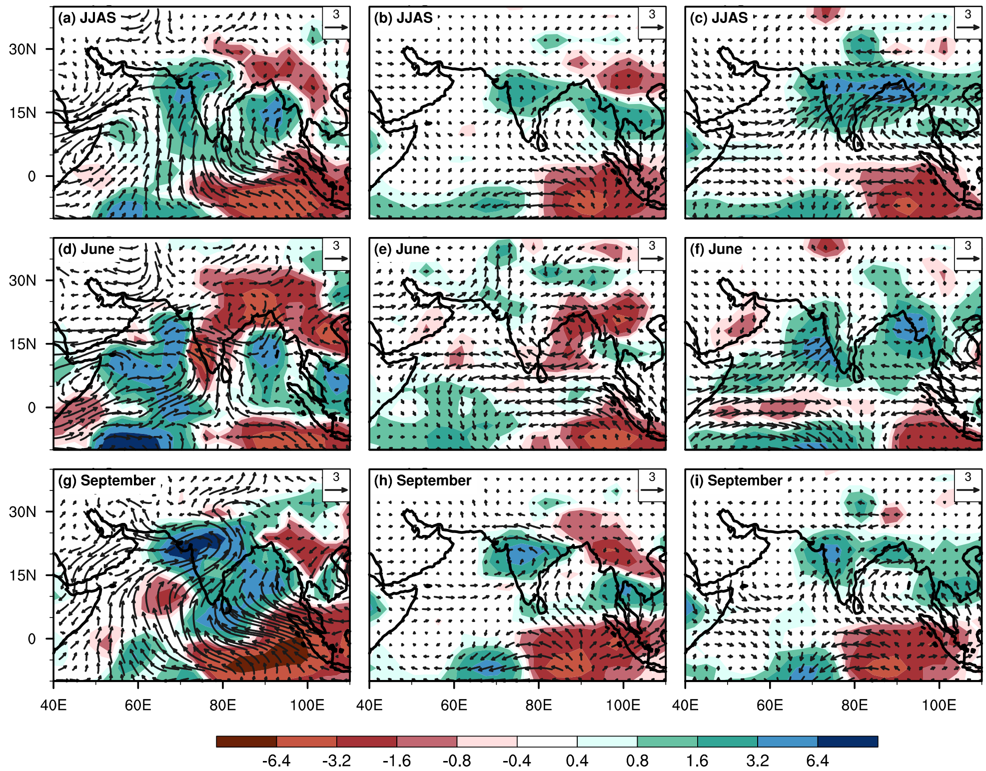

Fig. 2: (a, d, g) Observed GPCP rainfall anomaly (mm/day, shaded) and NCEP2 850 hPa wind anomaly (m/s, vectors) for June-September mean, June and September, respectively. (b,e,h) and (c,f,l) are the same as (a,d,g) but for IODglob and IODreg experiments, respectively. Shaded precipitation anomalies are significant at 90% level using a Student's t-test.

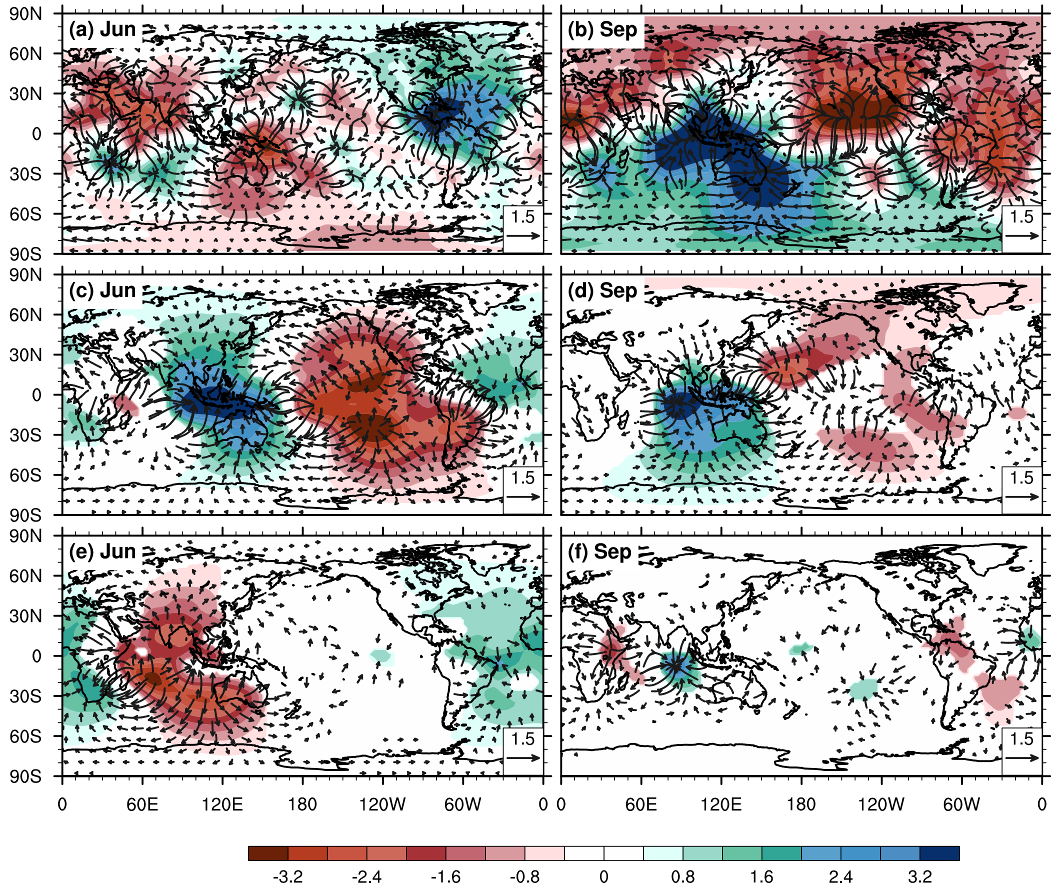

Fig. 3: (a,b) 200 hPa velocity potential (10^6 m^2 s^{-1}, shaded) and divergent wind (m s^{-1}, vectors) anomalies in 2019 June and September, respectively, based on the reanalysis. (c, d) and (e,f) are the same as (a,b) but for IODglob and IODreg experiments, respectively. Shaded velocity potential anomalies are significant at 90% level using a Student's t-test.

Figure 1.

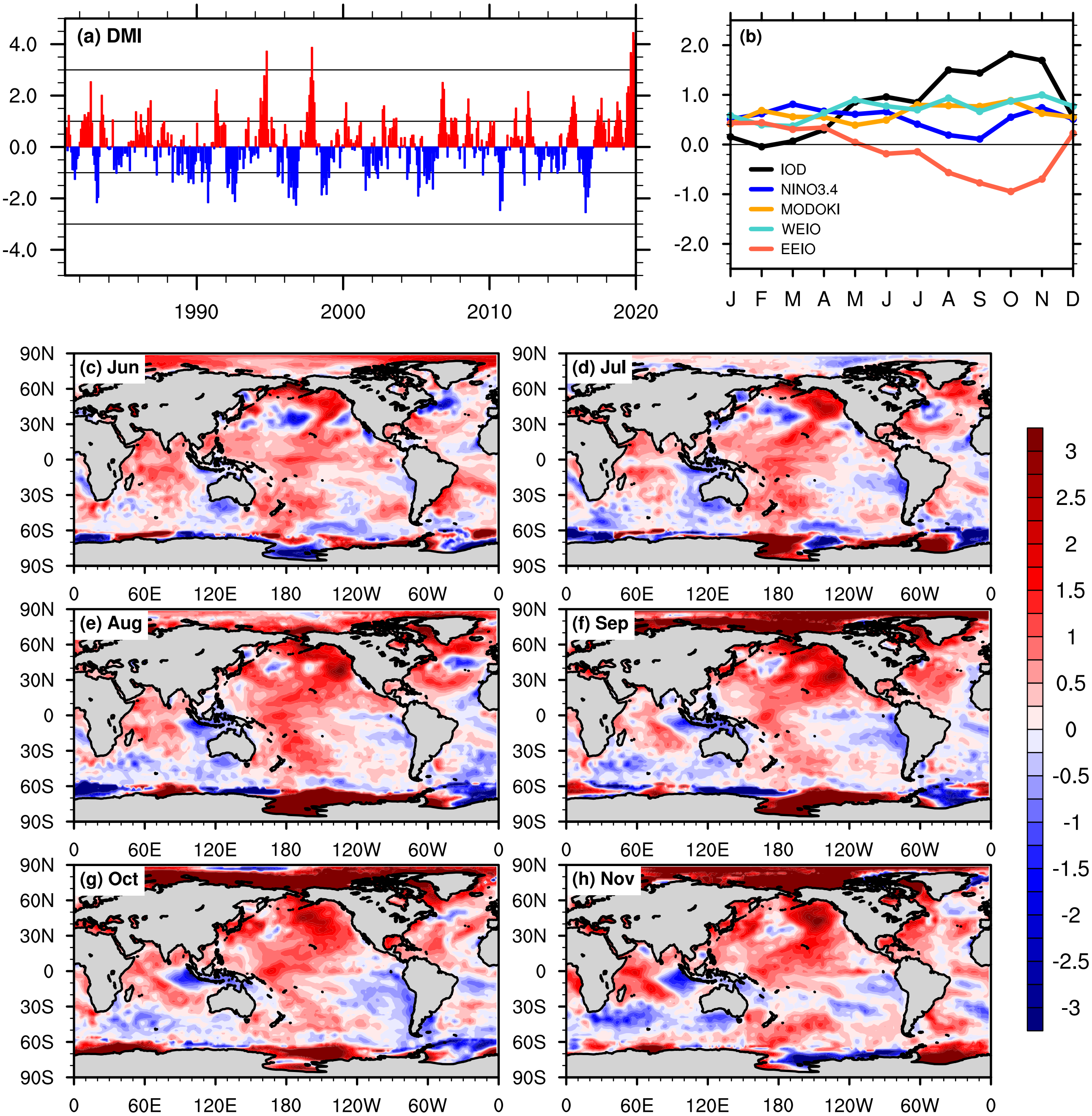

(a) DMI
4.0
2.0
0.0
-2.0
-4.0
1990
2000
2010
2020
(b)
2.0
1.0
0.0
-1.0
-2.0
IOD
NINO3.4
MODOKI
WEIO
EEIO
J F M A M J J A S O N D
(c) Jun
(d) Jul
(e) Aug
(f) Sep
(g) Oct
(h) Nov
90N
60N
30N
0
30S
60S
90S
0
60E
120E
180
120W
60W
0
3
2.5
2
1.5
1
0.5
0
-0.5
-1
-1.5
-2
-2.5
-3

Figure 2.

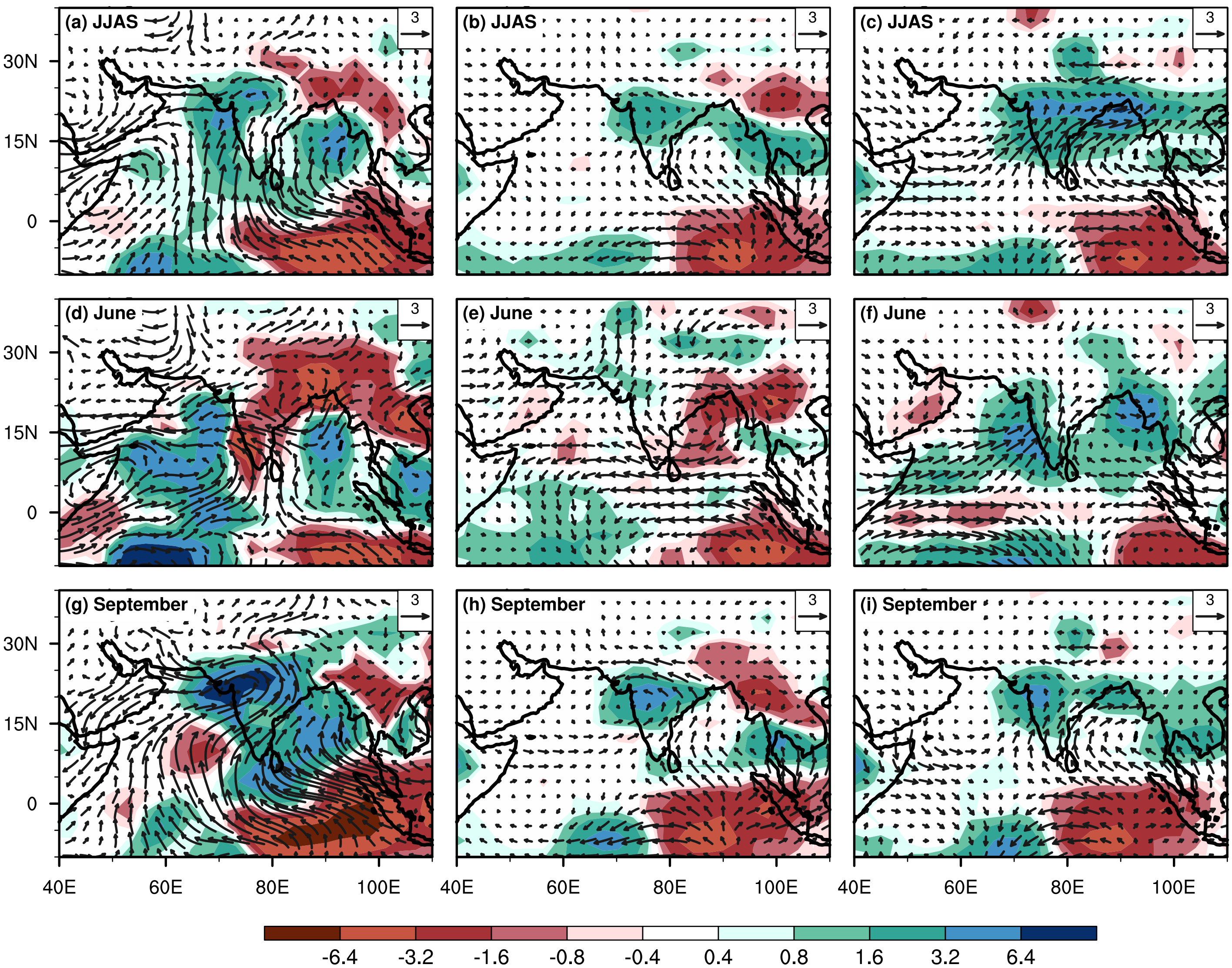

(a) JJAS
(b) JJAS
(c) JJAS
(d) June
(e) June
(f) June
(g) September
(h) September
(i) September
3
30N
15N
0
40E
60E
80E
100E
-6.4
-3.2
-1.6
-0.8
-0.4
0.4
0.8
1.6
3.2
6.4

Figure 3.

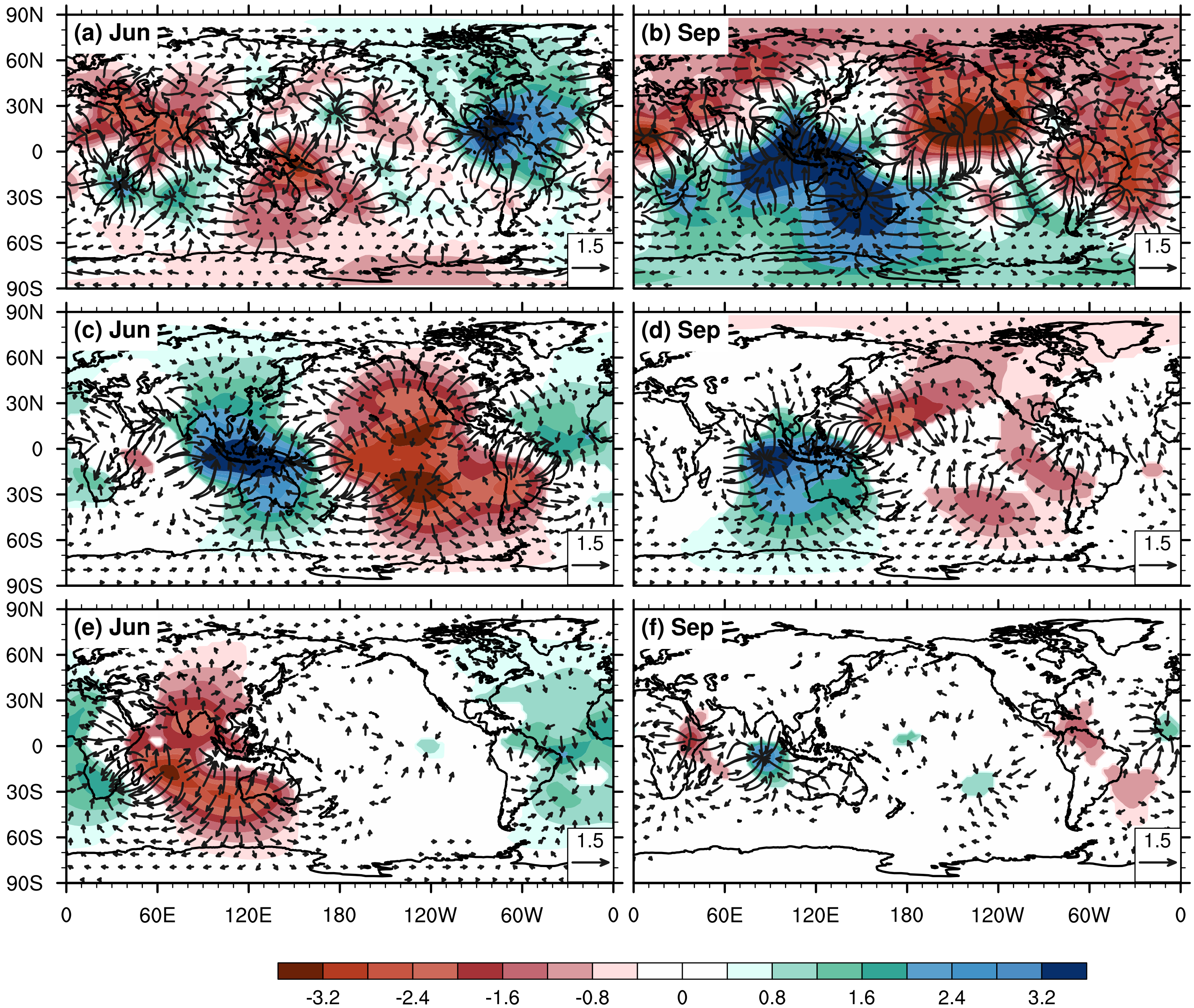

(a) Jun
(b) Sep
(c) Jun
(d) Sep
(e) Jun
(f) Sep
90N
60N
30N
0
30S
60S
90S
0
60E
120E
180
120W
60W
1.5
-3.2
-2.4
-1.6
-0.8
0.8
1.6
2.4
3.2